PHYSICAL REVIEW B, VOLUME 64, 121407(R)

Chirality-selective Raman scattering of the *D* mode in carbon nanotubes

J. Maultzsch, S. Reich, and C. Thomsen
Institut für Festkörperphysik, Technische Universität Berlin, Hardenbergstrasse 36, 10623 Berlin, Germany
(Received 16 June 2001; published 11 September 2001)

We show that *D*-mode Raman scattering in single-walled carbon nanotubes is due to a double-resonant Raman process. The unusual shift of the *D*-mode frequency with excitation energy is even expected for a single nanotube. The magnitude of the shift and the *D*-mode frequency depend strongly on the tube's diameter and chirality. Only tubes with $(n_1-n_2)/3n$ integer contribute to the *D*-mode spectrum because of the particular electronic structure of carbon nanotubes.

DOI: 10.1103/PhysRevB.64.121407 PACS number(s): 78.30.−j, 63.22.+m, 78.30.Na, 71.20.Tx

The Raman spectra of carbon nanotubes have been widely studied in first and second-order scattering. The observed first-order Raman modes are usually divided into low-energy modes at ≈ 200 cm^{-1} and high-energy modes at ≈ 1600 cm^{-1} (so-called *G* mode). Similar to graphite, the Raman spectra exhibit an additional peak around 1350 cm^{-1}, which cannot be attributed to a Raman-active Γ-point vibration. It has been known for long that this so-called *D* mode in graphite is disorder induced and corresponds to an optical phonon near the *K* point of the Brillouin zone.[1,2] Additionally and for a long time a mystery, in both materials the frequency of the *D* mode depends on excitation energy.[3,4] Frequency shifts of the *D* mode in carbon nanotubes of 38 cm^{-1}/eV, 53 cm^{-1}/eV for single-walled and 43 cm^{-1}/eV for multi-walled tubes have been reported.[5,6,4] The same holds for the second-order peak D^* (sometimes referred to as G'), which occurs at twice the frequency of the *D* mode and shifts by about twice the rate with excitation energy. Recently, the excitation-energy dependence of the *D* mode in graphite has been explained successfully as due to defect-induced, double-resonant Raman scattering.[7] Because of their related electronic structure the question arises whether a similar mechanism is present in carbon nanotubes as well.

In this paper we apply the double-resonance model to carbon nanotubes. Although the origin of the *D* mode is essentially the same as in graphite, we find that the one-dimensional electronic band structure in nanotubes strongly alters the double-resonance condition. Only in tubes with a particular condition for (n_1,n_2) we find the *D* mode, which agrees with recent experimental findings. Moreover, we propose that the *D* mode of single tubes, in general, consists of two peaks, their separation depending on excitation energy.

Carbon nanotubes are classified into metallic tubes if $(n_1-n_2)/3$ is integer and semiconducting tubes otherwise, where n_1 and n_2 are the components of the chiral vector. Indeed the electronic density of states in first-order approximation is the same for all metallic and all semiconducting tubes and depends only on diameter.[8] The details of the electronic band structure, though, in particular, the wave vectors k_S at which the singularities in the density of states appear, depend on a stronger condition for n_1 and n_2. In all semiconducting tubes the singularities for optical transitions in the range of visible light are at the Γ point of the Brillouin zone, i.e., $k_S=0$. Also in some metallic tubes k_S is at the Γ point, as in metallic zigzag tubes ($n_1/3$ integer and $n_2=0$). In general, $k_S=0$ for all tubes with $(n_1-n_2)/3n$ not being an integer ($R=1$), where n is the greatest common divisor of n_1,n_2. For tubes with integer $(n_1-n_2)/3n$ ($R=3$), the singularities in the density of states occur near $2\pi/3a$. All armchair tubes belong to this category; they additionally exhibit a crossing of valence and conduction bands at the Fermi wave vector $k_F=2\pi/3a$.[9]

For the calculation of a double-resonant Raman process the usual assumption that resonances are governed by the joint density of electronic states is no longer valid. Instead the full electronic dispersion has to be considered. We will show that the classification into $R=3$ and $R=1$ divides the tubes into those where one expects and does not expect the *D* mode, respectively. We start our investigation by considering armchair tubes, which are most familiar from the literature. After that we extend our model to general chiral tubes.

In armchair tubes optical transitions between the valence and conduction band in the range of visible light occur near $k_F=2\pi/3a$. Optical transitions between the bands which cross at $k_F=2\pi/3a$ are forbidden by selection rules. A defect-induced Raman process with two resonant transitions is then possible as shown in Fig. 1. The incoming photon resonantly excites an electron-hole pair near k_F (1), and the electron is resonantly scattered by a phonon across the Γ-point to $\approx -k_F$ (2). The electron is scattered back elastically by a defect to a virtual state (3), and the electron-hole pair recombines Eq. (4). For a given incoming resonance only a unique combination of phonon energy $\hbar\omega_{ph}$ and phonon wave vector q fulfills the double-resonance condition. The phonon wave vector q involved in the above process is $|q|\approx 2k_F=4\pi/3a=:q_0$. In zone folding this corresponds to a phonon mode originating from the *K* point of graphite and hence yields a phonon energy in the range of the *D* mode. If the excitation energy is increased, the incoming (or, alternatively, outgoing) resonance occurs at a greater distance from k_F. Therefore, the phonon wave vector leading to the second resonant transition becomes smaller or larger, depending on which side of the minimum the electron-hole pair was excited, see Fig. 1. As there is a minimum in the optical phonon dispersion at $q_0=4\pi/3a$, the phonon energy increases if the phonon wave vector moves away from q_0.

We calculate the Raman cross section for defect-induced scattering, which is given by fourth-order time-dependent perturbation theory:[10]

$$|K_{2f,10}|^2 = \left| \sum_{a,m} \frac{\mathcal{M}}{(E_{\text{laser}} - E_{ai}^m - i\gamma)(E_{\text{laser}} - \hbar\omega_{ph} - E_{bi}^m - i\gamma)(E_{\text{laser}} - \hbar\omega_{ph} - E_{ci}^m - i\gamma)} \right|^2, \quad (1)$$

where a,b are the intermediate electronic states, E_{ai} (E_{bi}) is the energy difference of the initial electronic state i and the two intermediate states a (b), and γ is the reciprocal lifetime of the intermediate states. We assume the matrix elements $\mathcal{M}$ to be constant, but include the selection rules for optical absorption and electron-phonon coupling. The sum in Eq. (1) is taken over all possible intermediate states and bands m, where the band index m corresponds to the discrete states $k_\perp$ perpendicular to the tube axis originating from the periodicity along the cirumference of the tube. For the electronic dispersion we use the symmetry-based tight-binding approximation with an overlap integral $\gamma_0 = 2.9$ eV.[11] We choose the incoming and outgoing light as polarized parallel to the tube axis (z) since this configuration was found to contribute most of the Raman signal in single-walled nanotubes.[12–14] For other scattering geometries our results do not change fundamentally. The Δm selection rule for z-polarized optical transitions is $\Delta m = 0$,[15] and the electron can only be scattered by a phonon within the same band. Therefore only phonons with band index $m = 0$ (A_{1g} symmetry at the Γ-point) are allowed. If the phonon wave vector $q > \pi/a$, the band $m = 0$ changes into $m = n$, because m is not conserved at the zone boundary.[16] This is depicted for the optical-phonon dispersion in armchair tubes in Fig. 1 (bottom); only the bands $m = 0,n$ are shown. The armchair $m = n$ band corresponds to the graphite phonons in the $\Gamma - K - M$ direction with $q \in]\pi/a, 2\pi/a]$ and thus contains the K point of graphite. For the phonon dispersion we use a model dispersion adapted to experimental and calculated values of the Γ and K-point frequencies,[17] which additionally reflects the symmetry of the hexagonal Brillouin zone of graphene.

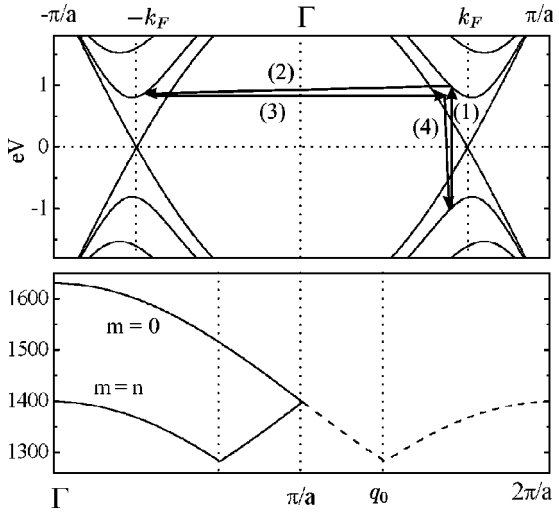

FIG. 1. Top: Defect-induced, double-resonant Raman process in the electronic band structure of a (10,10) tube. The electronic energies are given in eV. In the energy range of visible light an electron-hole pair is excited near $k_F = 2\pi/3a$ and scattered by a phonon across the Γ point. For a resonant transition the phonon wave vector is $\approx 4\pi/3a$. The electron is elastically scattered back by a defect and the electron-hole pair recombines. Bottom: Optical phonon dispersion bands $m = 0$ and $m = n$ as obtained by zonefolding from graphite (solid line). The minimum at $2\pi/3a$ of the $m = n$ band corresponds to the K-point phonon in graphite (dashed line: K-point at $4\pi/3a$ and M-point at $2\pi/a$).

In Fig. 2 we show the Raman spectra calculated with Eq. (1) for an (11,11) tube at three different excitation energies. The full calculated spectrum is displayed in the inset. We find a peak in the frequency range of the D mode, which is clearly dependent on the laser energy. Evidently our calculations reproduce the experimentally observed D mode. The calculated D mode is not symmetric and actually consists of two close together peaks. Their separation depends on the excitation energy; the smaller peak which appears as a shoulder on the low-frequency side shifts with excitation energy across the main peak. There are three reasons for this double-peak structure: the minimum of the electronic bands is shifted from $k_F = 2\pi/3a$, both the electron and phonon dispersion are not exactly symmetric around the minimum, and incoming and outgoing resonance yield a slightly different D-mode energy. The first two reasons account for the asymmetry of the peaks and their separation depending on excitation energy. Incoming and outgoing resonances are not resolved in our calculated spectra, but become visible when the dispersions are modified to be symmetric around the minima.

In Fig. 3 (top) the calculated frequency of the D mode is shown for a (10,10) and an (8,8) tube as a function of excitation energy. The frequency shifts of the D mode are 42 cm^{-1}/eV for the main peak and 76 cm^{-1}/eV for the low-

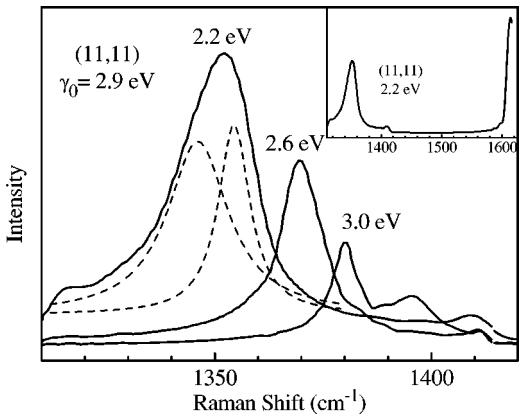

FIG. 2. Calculated D mode of the (11,11) tube (diameter 1.49 nm) at three different laser energies. The reciprocal lifetime of the electronic states is $\gamma = 0.1$ eV. The dashed lines are a fit by two Lorentzians. The small shoulder above 1400 cm^{-1} originates from the phonon density of states at the phonon wave vector which corresponds to the M point of graphite. The complete first-order spectrum is shown in the inset.

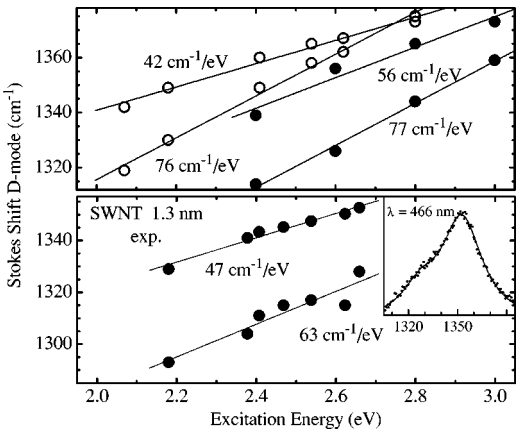

FIG. 3. Top: Calculated shift of the *D* mode as a function of excitation energy for the (10,10) tube (open circles) and the (8,8) tube (solid circles). The diameters of the tubes are 1.36 nm and 1.09 nm for the (10,10) and the (8,8) tube, respectively. For the (11,11) tube (not shown) we obtained a shift of the D-mode peaks of 35 cm^{-1}/eV and 65 cm^{-1}/eV. Bottom: Experimental shift of the *D* mode of nanotubes with a mean diameter of 1.3 nm. The solid lines are linear fits to the data points. Their slope is given next to the lines.

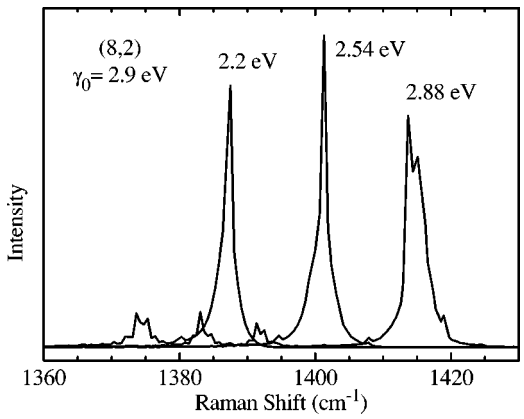

FIG. 4. Calculated *D* mode of an (8,2) tube at three different laser energies. The (8,2) tube has a diameter of 0.72 nm and $R=3$. The main peak shifts by 40 cm^{-1}/eV and the smaller peak by 27 cm^{-1}/eV. Note that the reciprocal lifetime $\gamma=0.05$ eV is smaller than in the calculation for the (11,11) tube, Fig. 2.

energy shoulder in the (10,10) tube and 56 cm^{-1}/eV and 77 cm^{-1}/eV in the (8,8) tube, respectively. For comparison we show in Fig. 3 (bottom) the experimentally obtained *D*-mode shift of unoriented single-walled nanotubes with a mean diameter of 1.3 nm.[18] In the inset the *D* mode at a laser energy of 2.66 eV is shown. Similar to our calculations, the *D* mode consists of a main peak with a shoulder on the low-energy side. The shifts of the two peaks are 47 cm^{-1}/eV and 63 cm^{-1}/eV. The calculated slope of the energy shift as well as the double-peak structure are in excellent agreement with the experiments.

In our calculations, the energy shift of the main peak increases with decreasing tube diameter whereas the absolute energies decrease. This is easily understood from the double-resonance process in Fig. 1. For smaller diameters the energy separation between valence and conduction band is larger. Therefore, at a given excitation energy a resonant transition occurs closer to the conduction-band minimum. First, this requires a phonon wave vector closer to q_0 for the second resonant transition which leads to a smaller phonon energy. Second, the slope of the electron dispersion is smaller near the conduction-band minimum. The wave vector of the initial state as well as the phonon wave vector in the resonance process depend stronger on excitation energy than for a larger slope in the electron dispersion. The same effect occurs if the overlap integral γ_0 is varied; with decreasing γ_0 the excitation-energy dependence of the *D* mode increases, but the absolute frequencies of the *D* mode are smaller.

The calculations discussed so far are for Stokes scattering. In anti-Stokes scattering we find the *D*-mode frequencies to be by ≈ 13 cm^{-1} higher than in the Stokes spectra. Again this up-shift follows from the double resonance. At a given excitation energy the phonon required for the second resonant transition is at a greater distance from q_0 than in Stokes scattering and therefore has a higher frequency. Experimentally, the difference between Stokes and anti-Stokes frequencies has been observed in graphite and is also expected for carbon nanotubes.[19] The second-order mode D^* is contained in the double-resonance model as well. The condition for the double resonance does not change in second order with respect to first order. Instead of defect scattering the excited electron (Fig. 1) is scattered twice by phonons with same energy but opposite wave vector and with a much larger Raman signal, because it is a Raman-allowed process. This leads to the D^* mode in second-order spectra at twice the frequency of the first-order *D* mode. Consequently, the frequency shift of the D^* mode as a function of excitation energy is twice the first-order shift, as observed experimentally.[4,5]

We now turn to the discussion of general tubes. For the presence of the *D* mode and its excitation-energy dependence it is essential that the minima of both the electron and optical-phonon dispersion are around 2/3 of the Brillouin zone as in armchair tubes. The electron wave vector k_i at which the resonant optical transition occurs and the phonon wave vector associated with the *D*-mode frequency both originate from the same part of the graphite Brillouin zone. The double-resonance process, on the other hand, involves a phonon wave vector $q \approx -2k_i$, see Fig. 1. The condition for double-resonant *D*-mode scattering is thus $q \approx -2k_i = k_i \pm 2\pi/a$, which directly yields $k_i = 2\pi/3a$ for the wave vector of the electronic transitions. As discussed in the beginning, only if $R=3$ the resonant optical transitions occur close to $2\pi/3a$. Therefore, we expect the *D* mode only for tubes with $R=3$. This is not a selection rule in the sense that scattering in $R=1$ tubes was forbidden by symmetry; but in $R=1$ tubes the double-resonance condition cannot be fulfilled by phonons with the *D*-mode frequency and wave vectors. Experimentally, a peak originating from a high phonon density of states might still be observed. It should, however, be weak in intensity and not show the excitation-energy dependence.

In Fig. 4 we show the calculated *D*-mode spectrum of the (8,2) tube ($R=3$) for three different excitation energies. We

find again a double-peak structure in the *D*-mode frequency range which shifts by 40 cm^{-1}/eV (main peak) and 27 cm^{-1}/eV (small peak on the low-energy side) with increasing excitation energy.

In zigzag tubes ($R=1$) the conduction-band minima are either at the Γ point or at the zone boundary; we do not expect the *D* mode at all. Moreover, in zigzag tubes the $m=0$ phonon band is above the frequency range of the *D* mode. Nevertheless, even if we modified the phonon frequencies with respect to graphite or included the E_{1g}, E_{2g} ($m=1,2$) phonon bands for other scattering configurations, we neither obtained the *D* mode nor the excitation-energy dependence by evaluating Eq. (1).

In the preceeding discussion we showed that only tubes with $R=3$ contribute to the *D* mode in first-order Raman spectra. The fact that particular single tubes do not show the *D* mode at all has been confirmed in first experiments on isolated single-walled nanotubes.[20] Raman spectra recorded from other single tubes in contrast exhibit a *D* mode which has nearly the same intensity as the high-energy *G* mode.[12] Another experimental finding is qualitatively explained by our calculations. Grüneis *et al.*[6] reported that the shift of the *D* mode in carbon nanotubes is not fully linear but superimposed by a sine-like function. The excitation-energy dependence of the *D* mode in our model is only linear if both dispersions are linear as well. A small deviation from the linearity is caused by the modified electron and phonon dispersion in nanotubes with respect to graphite. To study this behavior theoretically we need to include the modified phonon dispersion for specific carbon nanotubes and its dependence on the nanotube diameter, which will be done in a future work.

In conclusion, we showed that the *D* mode in the first-order Raman spectra of carbon nanotubes is due to a defect-induced, double-resonant Raman process. In our model the excitation-energy dependence of the *D* mode is a property of an individual tube. We calculated shifts of the *D* mode as a function of excitation energy between 35 and 56 cm^{-1}/eV depending on tube diameter and chirality, which agrees well with experimental data. The *D* mode of nanotubes exhibits a double-peak structure with the low-energy secondary peak shifting at a rate different from the main peak, which is found experimentally as well. The second-order mode *D** and the difference in Stokes and anti-Stokes scattering follow from the double-resonance model. Finally, we showed that all armchair tubes, most of the metallic chiral tubes (namely, those with $R=3$), and none of the zigzag or semiconducting chiral tubes show double-resonant *D*-mode scattering. Therefore, a single tube, which exhibits a strong *D* mode in the Raman spectra, can be identified as metallic.

This work was supported by the Deutsche Forschungsgemeinschaft under Grant No. Th 662/8-1.

[1] F. Tuinstra and J. L. Koenig, J. Chem. Phys. **53**, 1126 (1970).
[2] R. J. Nemanich and S. A. Solin, Phys. Rev. B **20**, 392 (1979).
[3] R. P. Vidano, D. B. Fischbach, L. J. Willis, and T. M. Loehr, Solid State Commun. **39**, 341 (1981).
[4] J. Kastner, T. Pichler, H. Kuzmany, S. Curan, W. Blau, D. N. Weldon, M. Delamesiere, S. Draper, and H. Zandbergen, Chem. Phys. Lett. **221**, 53 (1994).
[5] C. Thomsen, Phys. Rev. B **61**, 4542 (2000).
[6] A. Grüneis, M. Hulman, C. Kramberger, T. Pichler, H. Peterlik, H. Kuzmany, H. Kataura, and Y. Achiba, in *Proceedings of the XV International Winterschool on the Electronic Properties of Novel Materials*, edited by H. Kuzmany, J. Fink, M. Mehring, and S. Roth (AIP, Melville, New York, in press).
[7] C. Thomsen and S. Reich, Phys. Rev. Lett. **85**, 5214 (2000).
[8] J. W. Mintmire and C. T. White, Phys. Rev. Lett. **81**, 2506 (1998).
[9] M. Damnjanović, T. Vuković, and I. Milošević, Solid State Commun. **116**, 265 (2000).
[10] R. M. Martin and L. M. Falicov, in *Light Scattering in Solids*, edited by M. Cardona, Topics in Applied Physics Vol. 8 (Springer, Berlin, 1983), p. 91.
[11] M. Damnjanović, T. Vuković, and I. Milošević, J. Phys. A **33**, 6561 (2000).
[12] G. S. Duesberg, I. Loa, M. Burghard, K. Syassen, and S. Roth, Phys. Rev. Lett. **85**, 5436 (2000).
[13] A. Jorio, G. Dresselhaus, M. S. Dresselhaus, M. Souza, M. S. S. Dantas, M. A. Pimenta, A. M. Rao, R. Saito, C. Liu, and H. M. Cheng, Phys. Rev. Lett. **85**, 2617 (2000).
[14] S. Reich, C. Thomsen, G. S. Duesberg, and S. Roth, Phys. Rev. B **63**, R041401 (2001).
[15] I. Božović, N. Božović, and M. Damnjanović, Phys. Rev. B **62**, 6971 (2000).
[16] N. Božović, I. Božović, and M. Damnjanović, J. Phys. A **18**, 923 (1985).
[17] D. Sánchez-Portal, E. Artacho, J. M. Soler, A. Rubio, and P. Ordejón, Phys. Rev. B **59**, 12 678 (1999).
[18] Our samples were arc-discharge grown single-walled nanotubes. The Raman spectra were excited with an Ar^+Kr^+ laser, dispersed with a triple-subtractive monochromator (DILOR XY) and detected with a charge coupled device.
[19] P. H. Tan, Y. M. Deng, and Q. Zhao, Phys. Rev. B **58**, 5435 (1998).
[20] G. S. Duesberg, I. Loa, K. Syassen, W. Blau, and S. Roth, in *Proceedings of the XV International Winterschool on the Electronic Properties of Novel Materials* (Ref. 6).